Journal of Current Science and Technology, September-December 2024 Vol. 14 No. 3, Article 72

ISSN 2630-0656 (Online)

Cite this article: Suwodjo, R. A., & Ibrahim, Z. B. (2024). Modeling of an adaptive HHO gas controller based on fuzzy logic and polynomial function controls to improve engine torque of gasoline engine. *Journal of Current Science and Technology*, *14*(3), Article 72. https://doi.org/10.59796/jcst.V14N3.2024.72

Journal of Current Science and Technology

Journal homepage: https://jcst.rsu.ac.th

Modeling of an Adaptive HHO Gas Controller Based on Fuzzy Logic and Polynomial Function Controls to Improve Engine Torque of Gasoline Engine

Raden Agustinus Suwodjo[1, 2, *] and Zulkifilie bin Ibrahim[1]

[1]Faculty of Electrical Technology and Engineering, Universiti Teknikal Malaysia Melaka, Melaka 76100, Malaysia
[2]Department of Electrical Engineering, Universitas Nasional, Jakarta 12520, Indonesia

[*]Corresponding author; E-mail: suwodjo@gmail.com

Received 13 April 2024; Revised 13 August 2024; Accepted 13 August 2024
Published online 1 September 2024

Abstract

Typical hydrogen-hydrogen-oxygen gas (HHO) usage to improve gasoline engine performance refers to the fixed HHO flow rate method, providing 0.25–0.5 liters/minute of HHO for every 1000 cc engine size. However, the arising hypothesis expresses that the fixed HHO flow rate method does not optimally improve engine torque for various loads. The research objective is to propose an adaptive HHO gas controller that manages the HHO generator to produce an appropriate HHO flow rate for engine operation by adapting to load and engine speed variations. Hence, the engine torque improvement optimally occurs for various loads. The adaptive HHO controller combines fuzzy logic and polynomial function controls involving real-time engine data, such as mass airflow (MAF), air-fuel ratio (AFR), and the commanded AFR from the engine control unit (ECU), whose values vary with load and engine speed. A system simulation based on Matlab-Simulink investigates engine performance improvement due to the controller. The results show that the adaptive HHO flow rate due to the proposed adaptive HHO controller improves engine torque during small, medium, and big-loaded engine operations, respectively, by 1.5%–4.7%, 6.8%–26.8%, and 21.1%–72.8% depending on engine speed 2500 rpm–4000 rpm) and the commanded AFR (12.6–15.4). Conversely, under the same condition, the fixed HHO flow rate with 0.75 liters/minute HHO for a 1500 cc engine, used for comparison, improves the engine torque by 0%–0.6%, 0.3%–14.2%, and 9.3%–50.1%, respectively. The data show that the adaptive HHO controller provides better improvement. Moreover, the adaptive HHO controller improves engine thermal efficiency and reduces AFR error against the commanded AFR.

Keywords**:** *adaptive HHO; AFR; commanded AFR; fuzzy logic; gasoline engine; MAF; polynomial function*

List of Symbols:

V_{bat}	:	Battery voltage, 13.8 Volt DC;
V_{rev}	:	Reversible voltage for water splitting;
V_{act}	:	Voltage for electrode activation;
R_{KOH}	:	Internal resistance of KOH electrolytes;
R	:	Gas constant, 0.08206 liter.atm.K^{-1}.mole^{-1};
n	:	Mole amount of gas;
V	:	Volume;
T	:	Temperature;
P	:	Pressure;
I	:	Electric current of HHO generator;
J	:	Engine rotational moment of inertia;
σ	:	Spark advance;
N	:	Engine speed
$\dot{N}$	:	Engine speed acceleration
m_f	:	Mass of fuel in cylinder
m_a	:	Mass of air in cylinder
G_{MAF}	:	MAF gain
η	:	Engine thermal efficiency
u	:	Commanded AFR
D_{PWM}	:	PWM duty cycle;
Kp	:	Proportional coefficient
Ki	:	Integral coefficient
C_R	:	Compression ratio of engine
m_{HHO}	:	Mass of HHO gas in cylinder

List of Symbols (Cont.):

σ^* : Spark advance due to HHO usage;
m_{H2} : Mass of hydrogen in cylinder;
$\dot{m}_{H2}$: Hydrogen mass flow rate;
AFR^* : Air-fuel ratio due to fuel with HHO usage;
T^*_{eng} : Engine torque due to fuel with HHO usage;
$cAFR_{error}$: Change rate of AFR error;
$\dot{m}_{HHO}$: HHO mass flow rate
m_{O2} : Mass of oxygen in cylinder
$\dot{m}_{O2}$: Oxygen mass flow rate
T_{eng} : Engine torque
T_{load} : Load torque
AFR_{error} : AFR error

List of Abbreviations

AFR : Air-fuel ratio;
BTDC : Before-top-dead-center;
ECU : Engine control unit;
FIS : Fuzzy inference system;
HHO : Hydrogen-hydrogen-oxygen;
KOH : Potassium hydroxide;
LHV : Lower heating value;
MAF : Mass airflow;
PI : Proportional-integral;
PWM : Pulse width modulation;
CF : Correction factor of MAF gain;
OBD : On-board diagnostic;
rpm : Revolutions per minute;
DC : Direct current;

NB : Negative big (Fuzzy)
NM : Negative medium (Fuzzy)
NS : Negative small (Fuzzy)
ZO : Zero (Fuzzy)
PS : Positive small (Fuzzy)
PM : Positive medium (Fuzzy)
PB : Positive big (Fuzzy)
VVS : Very very small (Fuzzy)
VS : Very small (Fuzzy)
SM : Small (Fuzzy)
MD : Medium (Fuzzy)
BG : Big (Fuzzy)
VB : Very big (Fuzzy)
VVB : Very very big (Fuzzy)

1. Introduction

Previous research (Gad et al., 2024; Kultsum et al., 2024; Musmar, & Al-Rousan, 2011; Ridhuan et al., 2021; Sudarmanta et al., 2016) revealed that providing HHO gas into a gasoline engine increases engine performance, such as engine torque, power, and thermal efficiency, besides saving fuel consumption and decreasing toxic exhaust gas. Moreover, providing HHO gas to a gasoline engine improves the air-fuel ratio (AFR) of the engine (Abdullah, 2015; Musmar, & Al-Rousan, 2011), while AFR affects engine performance, including engine torque, power, thermal efficiency, fuel consumption, and exhaust gas (Bogdan et al., 2023; Khajepour et al., 2014). Another research revealed that improper HHO usage causes non-optimal engine performance enhancement (Madyira, & Harding, 2014). These phenomena encourage researchers to find an appropriate HHO flow rate for engine operation by managing the current of the HHO generator (El Soly et al., 2023; Ridhwan et al., 2023).

In practice, the typical usage of HHO follows Bob Boyce (Nabil, 2019), who prescribed 0.25 – 0.5 liters per minute of HHO for every 1000 cc engine size. His prescription adhered to the fixed HHO flow rate method regardless of load and engine speed. However, the emerging hypothesis suggests that the fixed HHO flow rate method does not optimally improve engine torque under various loads and engine speeds. Therefore, this research proposes a model of an adaptive HHO gas controller for a gasoline engine to improve engine torque for various loads. The adaptive HHO gas controller manages the HHO generator to produce a proper HHO flow rate for various engine operations regarding load and engine speed variations. Optimizing the HHO flow rate is essential because the hydrogen energy contained by HHO gas provides additional torque.

The simulation based on Matlab-Simulink integrates an HHO generator, a 1500 cc engine fueled by gasoline with HHO gas, and the adaptive HHO controller for observation. The research also compares engine torque improvement due to the fixed and adaptive HHO flow rates using the respective controller. Additionally, the research measures the torque of the gasoline engine without HHO as a baseline for comparison. Therefore, this research article describes the model of each subsystem before simulation.

The proposed adaptive HHO controller consists of the AFR controller, a proportional-integral (PI) current controller, and the electrolyte temperature limiter. The adaptive HHO gas controller works based on a combination of fuzzy logic and polynomial function controls involving real-time data of engine parameters. The involved engine parameters include MAF, AFR, and the commanded AFR issued by ECU

(Na et al., 2021), whose values vary with load and engine speed.

The novelty of the proposed HHO gas controller lies in its ability to adapt HHO supplementation for a gasoline engine to load and engine speed variations, thereby improving engine torque, AFR error, and engine thermal efficiency more than those provided by the fixed HHO flow rate method for any load and engine speed. It also means that the novelty of the proposed adaptive HHO gas controller improves the existing flaws of the fixed HHO flow rate method adhered to by many researchers in practice, which the existing method does not make the engine torque improvement optimal for engine speed and load variations.

2. Objectives

The research objective is to propose a model of an adaptive HHO gas controller, which controls the HHO generator to generate a proper HHO flow rate for gasoline engine operation by adapting to load and engine speed variations. Thus, engine torque improvement occurs optimally during operation under various loads.

3. Materials and methods

A simulation based on Matlab-Simulink investigates the performance of the adaptive HHO controller in improving gasoline engine torque. The investigation involves an HHO generator, a 1500 cc four-stroke four-cylinder gasoline engine fueled by gasoline and HHO, and the adaptive HHO controller. This research also compares engine torque improvements resulting from the fixed and adaptive HHO flow rates using the respective controllers. Therefore, this section describes the system configuration of the fixed and adaptive HHO flow rate generations, the model of each subsystem, and the simulation steps.

3.1 System Configuration

Figures 1 and 2 show block diagrams of the fixed and adaptive HHO flow rate generation for a gasoline engine, respectively.

Figure 1 shows the model of the fixed HHO flow rate generation for a gasoline engine, involving the PI current controller, the HHO generator, the engine fueled by gasoline with HHO, and the PI engine speed controller. The PI current controller provides a proper PWM voltage to the HHO generator, ensuring that the current is suitable for producing the required HHO (Baltacıoğlu, 2019; Sudarmanta et al., 2016). The HHO mass flow rate generation proportionally depends on the current of the HHO generator. The PI current controller maintains the actual current of the HHO generator precisely at the reference current set by the user (Huang, 2023). Setting the reference current determines the HHO mass flow rate for improving engine performance. However, if the electrolyte temperature is over 60°C, the electrolyte temperature limiter asks the PI current controller to shut down its PWM voltage output. As a result, the HHO generator safely produces pure HHO instead of water vapor (Conker, 2019; Sudarmanta et al., 2016). Besides, the system uses a PI engine speed controller, which regulates the throttle angle of the engine to keep the engine speed stable on the setpoint determined by the user during investigation.

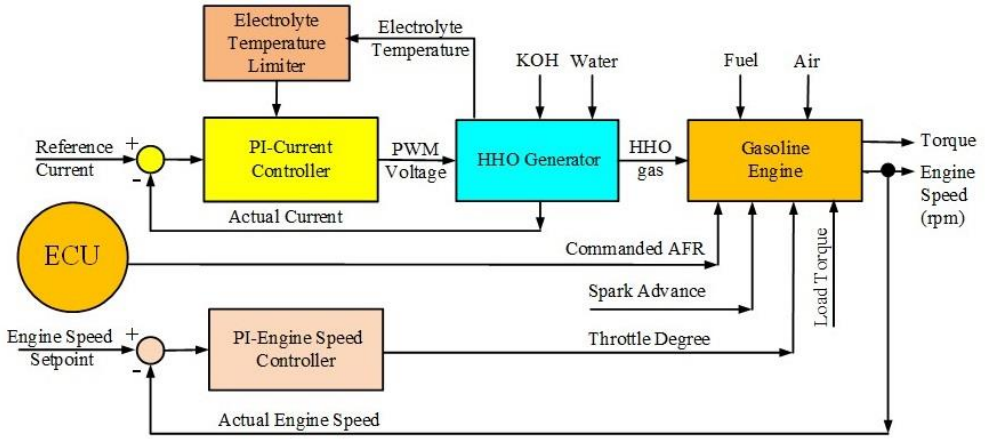

Figure 1 Block diagram of the fixed HHO flow rate generation for a gasoline engine

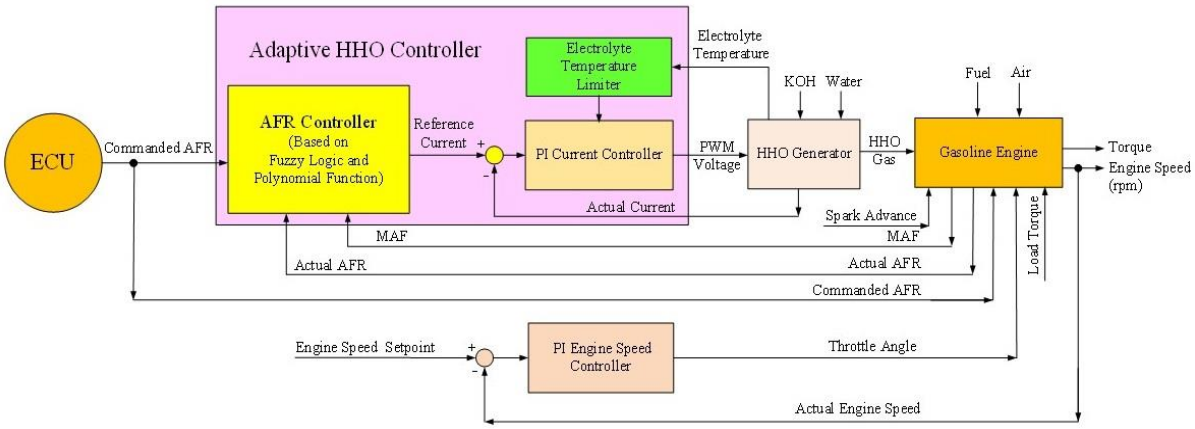

Figure 2 Block diagram of the adaptive HHO flow rate generation for a gasoline engine

Figure 2 shows the model of the adaptive HHO flow rate generation for a gasoline engine, which is similar to Figure 1, except that the reference current is determined by an AFR controller. The AFR controller automatically determines the reference current for the PI current controller, which manages the current of the HHO generator in producing appropriate HHO for the gasoline engine working with various loads and engine speeds. The AFR controller works based on a combination of fuzzy logic and polynomial function to determine the reference current by utilizing real-time engine data, such as MAF, AFR, and the commanded AFR issued by ECU. As a result, the new AFR of the engine matches the commanded AFR after receiving the appropriate HHO flow rate, optimizing engine torque for various operations. The commanded AFR is a target value of the engine's AFR determined by ECU based on engine speed and load.

Previous research (Khajepour et al., 2014; Bai, 2013) revealed that a gasoline engine operating at an AFR of 12.6 generates the maximum power but consumes more fuel. In contrast, operating at an AFR of 15.4 causes the engine to consume the least fuel but produce less power. Theoretically, a gasoline engine reaches the optimal power and fuel consumption if the engine operates at the stoichiometric AFR (AFR = 14.7). Therefore, this research focuses on observing the effect of the HHO controller on a gasoline engine operating at AFRs of 12.6, 14.7, and 15.4.

3.2 HHO generator

HHO generator splits water through electrolysis process using electric current and potassium hydroxide (KOH) as a catalysts to produce HHO gas, which consists of hydrogen (H_2) gas and oxygen (O_2) gas in a 1:8 mass ratio (Muthu et al., 2022; Newborough, & Cooley, 2021). KOH accelerates HHO generation more effectively than other conventional catalysts, such as sodium hydroxide (NaOH) and sodium bicarbonate ($NaHCO_3$) (Muthu et al., 2022). Moreover, the HHO mass flow rate is the sum of hydrogen and oxygen mass flow rates**.** An HHO generator has some cells in series that produce HHO gas. According to Faraday's law of electrolysis (Marefatjouikilevaee et al., 2023), the HHO mass flow rate ($\dot{m}_{HHO}$) produced by the six-cell HHO generator is given by Equation (1):

$$\dot{m}_{HHO}=0.00056 \cdot I \quad (1)$$

the current (I) for the six-cell HHO generator is given by Equation (2) (Marefatjouikilevaee et al., 2023; Niroula et al., 2023):

$$I = \left(\frac{V_{bat}}{6} - V_{rev} - V_{act}\right) \cdot D_{PWM} / R_{KOH} \quad (2)$$

where V_{bat} = 13.8 Volt DC supply from battery;

V_{rev} = reversible voltage for water splitting, which the value is 1.229 Volt at 25°C and 1 bar as a standard condition (Marefatjouikilevaee et al., 2023);

V_{act} = the voltage for electrode activation;

R_{KOH} = the internal resistance of KOH electrolytes depending on electrolyte concentration and temperature (Gambou et al., 2022; Lim et al., 2022).

Equation (2) shows that varying the PWM duty cycle (D_{PWM}) can provide the required electric current for the HHO generator. This phenomenon is similar to the previous research results (Conker, & Baltacioglu, 2020; Sudarmanta et al., 2016).

If the required HHO flow rate is 0.75 Liters per minute at 50°C and 1 atm pressure, this rate is

equivalent to 0.75/60 = 0.0125 liters per second of HHO gas. By using a formula related to ideal gas (PV = nRT) with gas constant R = 0.08206 liter.atm.K^{-1}.$mole^{-1}$, n = mole amount of gas, T = temperature (K), P = pressure (atm), the 0.0125 liters per second of HHO gas flow rate at 50°C and 1 atm, is equivalent with the following HHO mole flow rate (Karn, & Demiroglu, 2023).

$$\text{Mole flow rate of HHO gas} = \frac{0.0125}{0.08206 \text{ x } (50+273.15)}$$
$$= 0.00047 \text{ moles/second.}$$

The mole ratio of hydrogen and oxygen in HHO gas is 2:1, so the mole flow rate of hydrogen is always 2/3 of the mole flow rate of HHO gas, and the mole flow rate of oxygen is always 1/3 of the mole flow rate of HHO gas. Additionally, the molar mass of hydrogen is 2 grams and the molar mass of oxygen is 32 grams. As a result, the mass flow rate of HHO gas ($\dot{m}_{HHO}$) can be calculated as follows:

$$\dot{m}_{HHO} = \underbrace{(2/3 \text{ x } 0.00047 \text{ x } 2)}_{\text{hydrogen}} + \underbrace{(1/3 \text{ x } 0.00047 \text{ x } 32)}_{\text{oxygen}}$$

$\dot{m}_{HHO}$ = 0.00564 gram/second

Thus, generating 0.75 liters per minute of HHO is equivalent to generating an HHO mass flow rate of 0.00564 grams/second. According to Equation (1), the HHO generator will consume (0.00564/0.00056) = 10.07 Amperes of electric current to generate 0.00564 grams/second of HHO gas.

3.3 Gasoline engine with HHO generator

A four-stroke gasoline engine completes the combustion process in two revolutions of the crankshaft through sequential cycles of intake, compression, power, and exhaust. Empirically, an engine using gasoline produces engine torque, as shown in Equation (3) (Namitha, & Shantharama, 2013; Setiadi et al., 2021):

$$T_{eng} = -181.3 + 379.36 \cdot m_a + 21.91 \cdot (A/F) - 0.85 \cdot (A/F)^2 + 0.26 \cdot \sigma - 0.0028 \cdot \sigma^2 + 0.027 \cdot N - 0.000107 \cdot N^2 + 0.00048 \cdot N \cdot \sigma + 2.55 \cdot \sigma \cdot m_a - 0.05 \cdot \sigma^2 \cdot m_a \quad (3)$$

where T_{eng} = Engine torque (Newton.meter; N·m);
A/F = Ratio of mass of air to mass of fuel, also named as AFR.

$$\text{AFR} = \frac{m_a}{m_f} \quad (4)$$

Then, subtracting the load torque from the engine torque results in engine speed acceleration shown in Equation (5):

$$J \cdot \dot{N}_{=T_{eng}} - T_{load} \quad (5)$$

However, previous research showed that HHO usage in gasoline engines causes engine torque to increase by about 5% − 32.4% (Yilmas, 2010; Abdullah, 2015; Sudarmanta et al., 2016). Moreover, other research (Elsemary et al., 2017; Sudarmanta et al., 2016) showed that decreasing the spark advance (degree before top-dead-center) and simultaneously providing HHO to the gasoline engine results in greater improvement in engine torque and other performance than providing HHO alone. These phenomena encourage the development of a new engine torque equation for an engine fueled by gasoline and HHO, as shown in Equation (6) instead of Equation (3).

Equation (6) shows that the engine torque due to HHO usage (T^*_{eng}) depends on a mixture of air, gasoline, and HHO gas consisting of hydrogen and oxygen.

$$T^*_{eng} = -181.3 + 379.36 \cdot (m_a + m_{O2}) + 21.91 \cdot (A/F^*) - 0.85 \cdot (A/F^*)^2 + 0.26 \cdot (\sigma^*) - 0.0028 \cdot (\sigma^*)^2 + 0.027 \cdot N - 0.000107 \cdot N^2 + 0.00048 \cdot N \cdot (\sigma^*) + 2.55 \cdot (\sigma^*) \cdot (m_a + m_{O2}) - 0.05 \cdot (\sigma^*)^2 (m_a + m_{O2}) + 120000 \cdot m_{H2} \cdot C_R/\pi \quad (6)$$

where C_R = Compression ratio of engine;
m_{H2} = Mass of hydrogen in cylinder;
T^*_{eng} = Engine torque due to fuel with HHO usage (Newton.meter);
A/F^* = Air-fuel ratio due to fuel with HHO usage, also named as AFR^*;
AFR^* is the modified equation for new AFR, as shown in Equation (7):

$$AFR^* = \frac{(m_a + m_{O2})}{(m_f + m_{H2})} \quad (7)$$

The proposed term ($120000\, m_{H2}.C_R/\pi$), as shown in Equation (6), represents the additional engine torque due to hydrogen energy during the engine's power cycle. The proposed term involves hydrogen energy (= lower heating value of hydrogen), whose value is 120000 joule/gram (Aghahasani et al., 2022), and the power cycle duration of an engine, whose value is ½ of the period of engine revolution. Then,

subtracting the load torque from the engine torque results in engine speed acceleration, as shown in Equation (8) (Namitha, & Shantharama, 2013):

$$J\cdot\dot{N}=\dot{T}^{*}_{eng}-T_{load} \quad (8)$$

An engine thermal efficiency (η) is the ratio of work output and energy input from fuel (Kultsum et al., 2024). Therefore, engine thermal efficiency using HHO gas supplementation can be elaborated as in Equation (9):

$$\eta=\frac{\text{Work output}}{\text{Energy input from fuel}}\text{ x }100\%$$

$$\eta=\frac{\text{Power output}}{\text{Gasoline flow rate}\cdot\text{LHV gasoline}}\text{ x }100\%$$

$$\eta=\frac{(T^{*}_{eng}-T_{load})\cdot N}{[\frac{(MAF+\dot{m}_{O2})}{AFR^{*}}-\dot{m}_{H2}]\cdot 43000}\text{x}100\% \quad (9)$$

where LHV gasoline = The lower heating value of gasoline = 43000 Joule/gram.

Equations (7) and (9) show that HHO supplementation in gasoline engine improves the engine's air-fuel ratio, thereby enhancing engine thermal efficiency.

Figure 4 shows the simulation model of the overall engine fueled by gasoline with HHO, developed by referring to the model of an engine without HHO, as shown in Figure 3 (The MathWorks Inc., 2024).

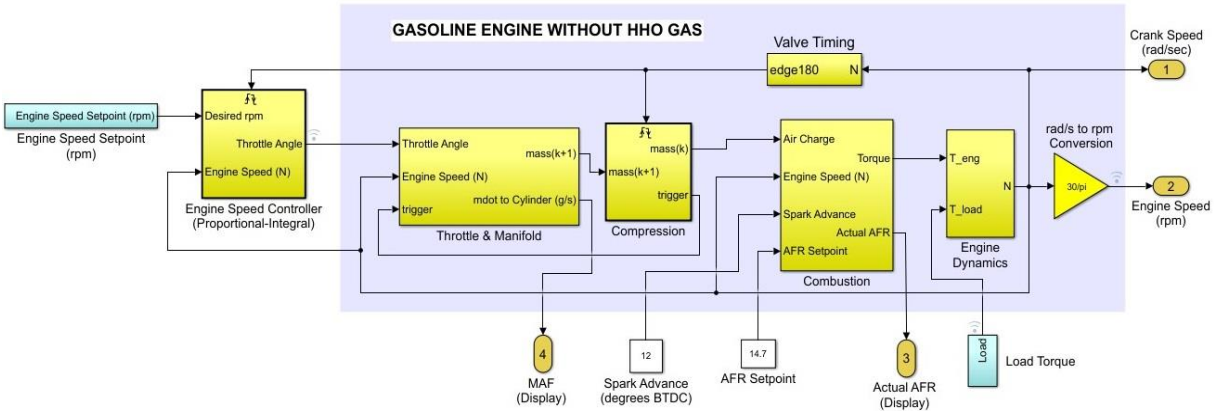

Figure 3 Model of four-cylinder four-stroke gasoline engine without HHO
Adapted from **"**Engine Timing Model with Closed Loop Control" by The MathWorks Inc., 2024, https://www.mathworks.com/help/simulink/slref/engine-timing-model-with-closed-loop-control.html

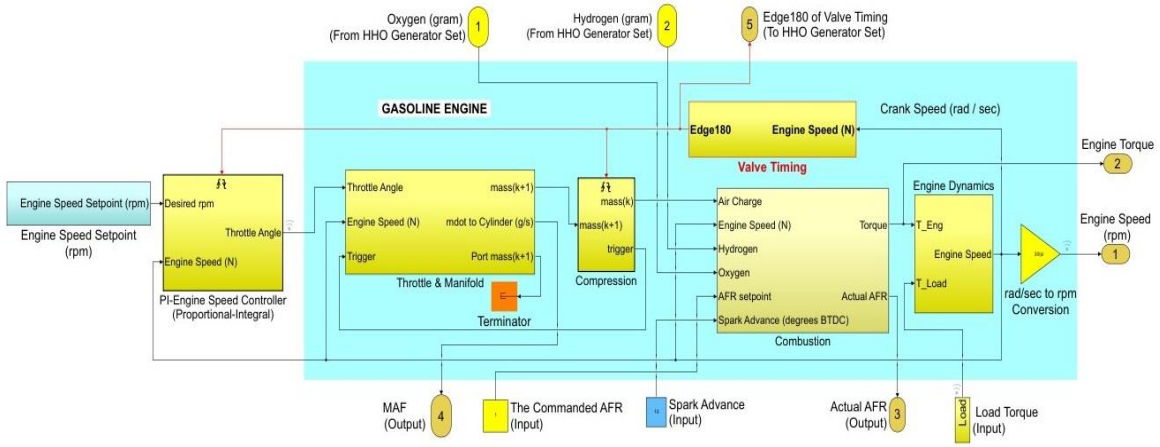

Figure 4 Model of four-cylinder four-stroke engine fueled by gasoline with HHO

3.4 Adaptive HHO controller

The proposed adaptive HHO controller manages the HHO generator's current based on a combination of fuzzy logic and polynomial function controls. As a result, the HHO generator generates a proper HHO flow rate for various engine operations. A control technique based on a combination of fuzzy logic and polynomial functions reduces the control design complexity (Conker, 2019) and minimizes the error of the results. The adaptive HHO controller consists of the AFR controller, the PI current controller, and the electrolyte temperature limiter.

3.4.1 AFR controller

The proposed AFR controller, as shown in Figure 5, generates a proper reference current for the PI current controller, which controls the current of the HHO generator to produce a proper HHO flow rate for engine operation.

The AFR controller generates an appropriate reference current by multiplying the basic current and the amplified mass airflow. The basic current value is derived from a fuzzy inference system (FIS) that incorporates the actual AFR from the engine and the commanded AFR from ECU. Meanwhile, the amplified mass airflow value is the MAF value normalized by 20 grams/second of maximum MAF and then multiplied by an MAF gain. Moreover, MAF gain and its correction factor depend on the commanded AFR value, as shown in Equations (10) and (11).

$$G_{MAF}=(-0.0097\cdot u^3+0.4638\cdot u^2-7.5954\cdot u+43.858)\cdot(1+CF) \quad (10)$$

$$CF=|0.005\cdot(-0.0871\cdot u^4+4.8542\cdot u^3-101.27\cdot u^2+936.22\cdot u-3235.6)| \quad (11)$$

where u = Commanded AFR; G_{MAF} = MAF gain; CF = Correction factor of MAF gain.

Figures 5 and 6 show the FIS input variables, which include AFR error (= AFR_{error}) and change rate of AFR error (= $cAFR_{error}$). The FIS output variable is the basic current, with a value ranging from 0 –14 Amperes. Moreover, the commanded AFR value is 12.0 – 16.0.

AFR error is the deviation of actual AFR against the commanded AFR, as shown in Equation (12), whereas the change rate of AFR error is the change of AFR error per time unit.

$$AFR_{error}=(AFR_{commanded}-AFR_{actual})/AFR_{commanded}\cdot 100\% \quad (12)$$

where AFR_{actual} = Actual AFR of the engine; $AFR_{commanded}$ = The commanded AFR issued by ECU; AFR_{error} = The deviation of actual AFR against the commanded AFR (%).

The AFR error variable's value ranges from 0 to 4% due to scaling by (10v + 2), where v is the previous AFR error value. The change rate of AFR error variable's value ranges from 0 to 4% per unit of time due to the scaling by (1000000000 w + 2), while w is the previous change rate of AFR error value. The value of the change of AFR error is positive or negative. The FIS utilizes abbreviations for the variable's value range, such as NB (Negative Big), PB (Positive Big), VVS (Very Very Small), and VVB (Very Very Big).

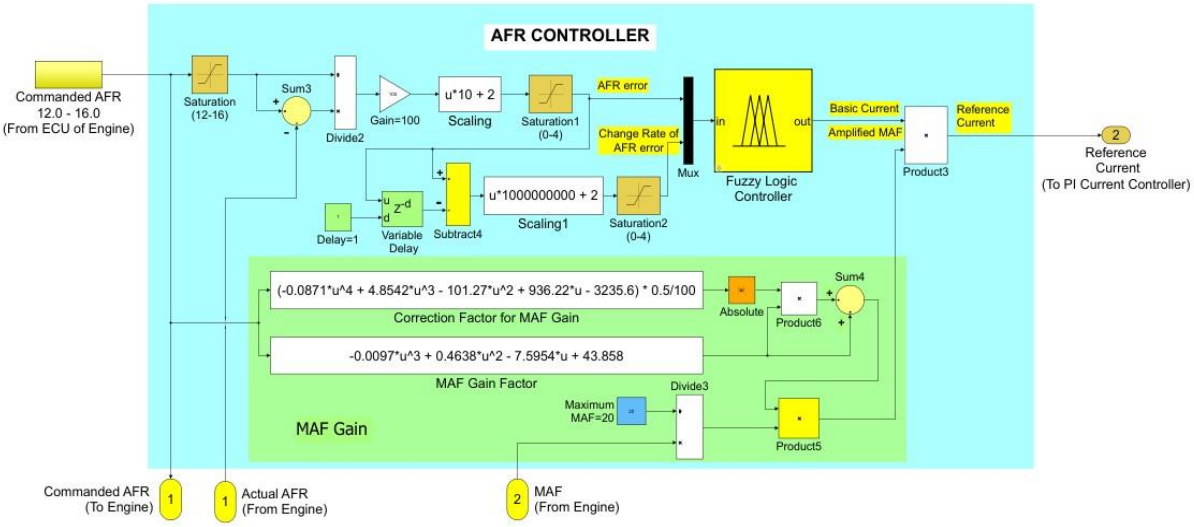

Figure 5 Model of the proposed AFR controller

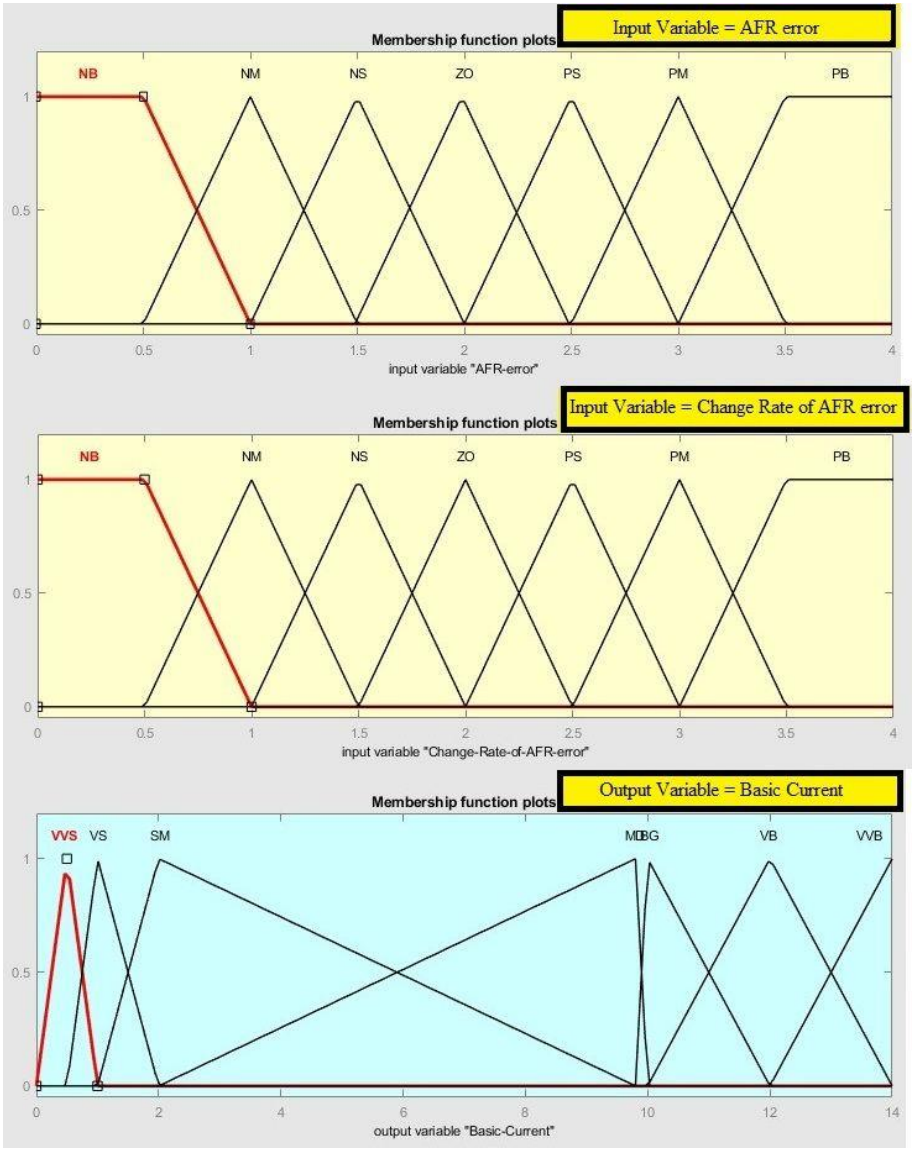

Figure 6 The Input and Output Variables in Fuzzy Inference System (FIS)

Table 1 Fuzzy Rules of the AFR Controller

		Change Rate of AFR error						
		NB	**NM**	**NS**	**ZO**	**PS**	**PM**	**PB**
AFR error	NB	VVB	VVB	VVB	VVB	VVB	VVB	VVB
	NM	VVB	VVB	VB	VB	VB	VB	VB
	NS	VB	VB	BG	BG	BG	BG	BG
	ZO	BG	BG	MD	MD	MD	MD	MD
	PS	VS	VS	VS	VS	VS	VS	VS
	PM	VS	VS	VS	VS	VS	VVS	VVS
	PB	VVS	VVS	VVS	VVS	VVS	VVS	VVS

Table 1 below presents the fuzzy rule of the AFR controller. It presents the correlation between the FIS input variables (AFR error and Change rate of AFR error) and the FIS output variable (Basic Current).

3.4.2 PI current controller and electrolyte temperature limiter

Figure 7 presents the proposed PI current controller model, which consists of a PI controller, a current-to-voltage converter, switches, and a PWM generator. The electrolyte temperature limiter is connected to the PI current controller and monitors the electrolyte temperature inside the HHO generator.

The PI current controller sends an appropriate PWM voltage to the HHO generator so that the current of the HHO generator is precisely the same as the reference current issued by the AFR controller for the required HHO flow rate. The PI current controller uses Kp = 0.05 and Ki = 10 coefficients for optimal overshoot, rise time, and 0.5% settle error. However, if the electrolyte temperature limiter sends a signal indicating an over 60°C in the electrolyte inside the HHO generator, the PI current controller shuts down the PWM voltage.

3.5 Simulation steps

First, the simulation using Matlab-Simulink runs for 18 seconds to measure the performance of a gasoline engine without HHO usage as the baseline measurement. The simulation refers to Figure 3, in which the engine operates with spark advance (degree before top-dead-center) = 12º and begins with the initial AFR = 0.1% higher than the commanded AFR, so the engine begins with less power. Moreover, the PI engine speed controller uses Kp = 0.5 and Ki = 0.1 coefficients. The measurements focus on the AFR error against the commanded AFR, the peak engine torque, and the engine thermal efficiency when the engine operates at idle speed and 2500 rpm starting at the 8th second. Moreover, the measurements are conducted when the engine runs using the commanded AFR = 12.6, 14.7, 15.4, with no load, small load (13.75 N·m, 25% of full load), medium load (27.5 N·m, 50% of full load), and big load (40 N·m, 72.8% of full load), alternately. Next, the measurements are repeated for 3000 rpm and 4000 rpm.

Second, the next simulation measures the AFR error against the commanded AFR, the peak engine torque, and the engine thermal efficiency of a gasoline engine due to the fixed HHO flow rate, following the same procedure as the first above, except that the engine operates with a spark advance of 10º to increase the engine torque. The system simulation refers to Figure 1, in which the engine operates with spark advance = 10º to increase the engine torque due to HHO usage. The PI current controller uses Kp = 0.05 and Ki = 10 coefficients. Besides, the setting of the reference current is 10.07 Ampere, so the HHO generator generates 0.75 liters per minute of HHO gas, the same as 5.635 x 10^{-3} gram/second of HHO gas for a 1500 cc engine size. The HHO flow rate refers to the typical practice, which uses 0.5 liters per minute of HHO flow rate for each 1000 cc engine size, as Bob Boyce prescribed (Nabil, 2019). Meanwhile, the 10.07 Ampere reference current setting refers to the calculation for generating 0.75 liters per minute of HHO gas at 50°C, 1 atm of pressure, as described in section 3.2 above.

Third, the subsequent simulation referring to Figure 2 measures the AFR error against the commanded AFR, the peak engine torque, and the engine thermal efficiency of a gasoline engine due to the adaptive HHO flow rate. The procedure is the same as in the second simulation, except that no reference current setting is required because the AFR controller automatically provides it to the PI current controller.

Finally, the research calculates the improvements of the AFR error against the commanded AFR, the engine torque, and the engine thermal efficiency of the gasoline engine using both fixed and adaptive HHO flow rates. Each improvement is measured against the engine's performance without HHO, which acts as a baseline of comparison.

4. Results and discussion

This section presents graphics of some parameters affecting engine performance when engine speed and load change.

4.1 Observation on parameters affecting the engine torque and engine thermal efficiency

Figure 8 below shows the MAF varying with load and engine speed, so the MAF value differed for each engine operation. MAF influences the mass of air inside the engine during combustion, which in turn affects engine torque, as shown in Equation (3) (Namitha, & Shantharama, 2013; Setiadi et al., 2021) and also affects the engine thermal efficiency, as shown in Equation (9).

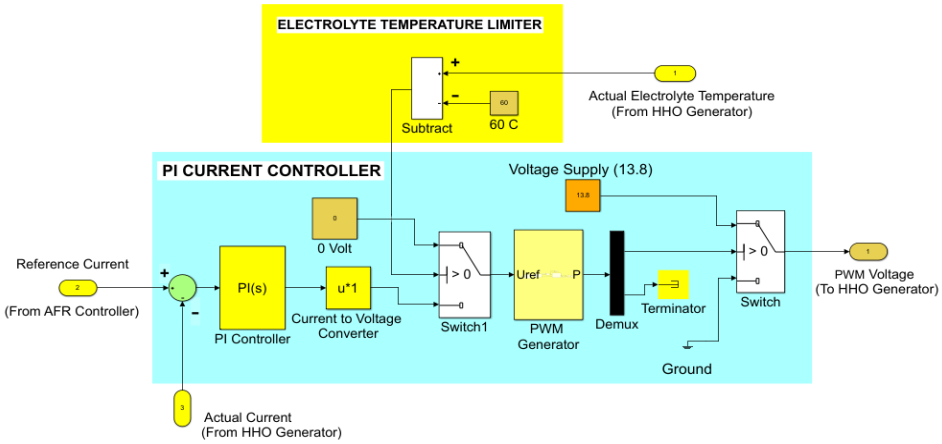

Figure 7 Model of the proposed PI current controller

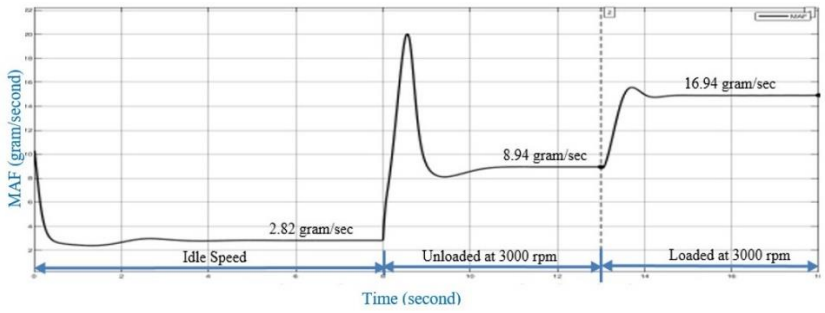

Figure 8 The change of MAF entering the engine due to engine speed and medium load

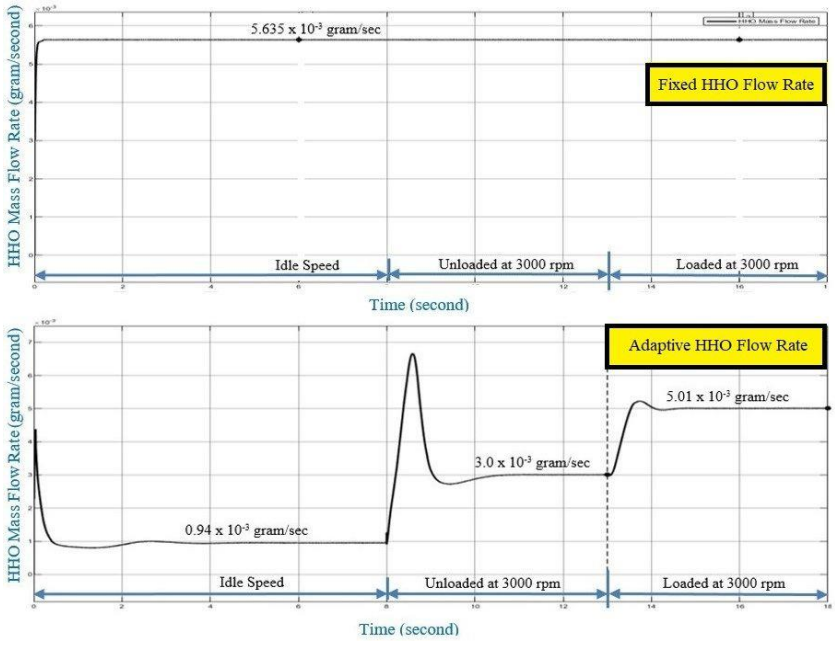

Figure 9 The fixed and adaptive HHO mass flow rates of the gasoline engine with a medium load at the commanded AFR = 14.7

Figure 9 below shows the fixed HHO mass flow rate (5.635 x 10^{-3} gram/second) generated by the system using 10.07 Ampere of the HHO generator's current regardless of load and engine speed variations. The user manually sets the reference current to obtain the required HHO mass flow rate.

In contrast, Figure 9 also shows an adaptive HHO mass flow rate due to the proposed adaptive HHO controller, which varies with load and engine speed, resulting in different HHO mass flow rates for each engine operation, such as idle speed, unloaded at 3000 rpm, and loaded at 3000 rpm. The variation in HHO flow rate occurred because the adaptive HHO controller takes into account the mass airflow (MAF) entering the engine, the actual AFR* of the engine, and the commanded AFR (= target of AFR) issued by the engine control unit (ECU). The adaptive HHO controller determines the required HHO flow rate using a combination of fuzzy logic and polynomial function controls, as section 3.4 described.

Figures 10 below show the actual AFR during the operation of the engines without HHO and using HHO. The actual AFR in the engine without HHO remains the same as the initial AFR, whose AFR error is 0.1 % against the commanded AFR. There is no improvement of steady AFR error in the gasoline engine without HHO.

In contrast, Figure 10 also shows that the gasoline engine using the adaptive HHO flow rate resulted in a zero steady AFR error against the commanded AFR for any engine operation, As shown in Equation (7), the new AFR (= AFR*) meets the commanded AFR (= target of AFR) if the amount of hydrogen and oxygen composing HHO gas is always proper for any engine speed and load variations. The zero steady AFR error achievement was successful because the adaptive HHO controller made the proper HHO flow rate for any engine operation by adapting to MAF, AFR*, and the commanded AFR, as described in section 3.4.

On the other hand, Figure 10 also shows the gasoline engine using the fixed HHO flow rate, which resulted in non-zero steady AFR error against the commanded AFR for any engine operation. Referring to Equation (7), the failure to achieve the commanded AFR occurred because of HHO over or under-supply. HHO oversupply and HHO undersupply made a lower AFR* and a higher AFR*, respectively. The lower AFR* causes more power but more fuel consumption. Meanwhile, higher AFR* causes less fuel consumption but less power.

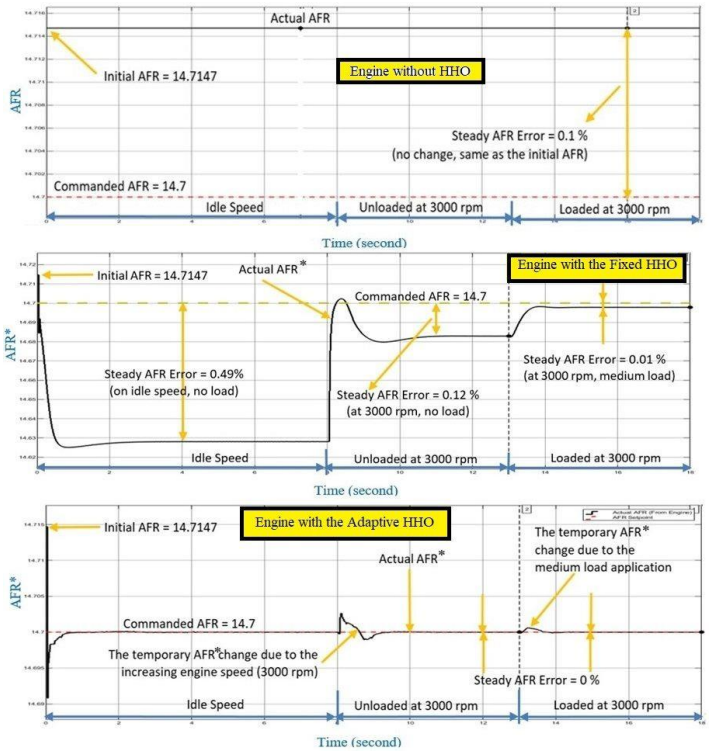

Figure 10 The actual AFR of gasoline engines without HHO, with the fixed and adaptive HHO flow rates at 3000 rpm, medium load, and the commanded AFR = 14.7

4.2 Improvement of the engine performance due to HHO usage

Figures 12 - 14 show a comparison of improvements in the gasoline engine performance due to the fixed and adaptive HHO flow rates at some engine speeds, loads, and commanded AFRs. The engine performance includes the AFR error against the commanded AFR, the peak engine torque, and the engine thermal efficiency. Improvement of engine performance due to the fixed and adaptive HHO flow rates, respectively, is calculated relative to the performance of engine without HHO, which acts as a baseline of comparison.

Improvements of AFR error against the commanded AFR and also engine thermal efficiency due to HHO usage refer to Equation (13):

$$\text{Improve}_{\text{Performance}} = \left| \frac{|\text{Performance}_{\text{HHO}}| - \text{Performance}_{\text{noHHO}}}{\text{Performaance}_{\text{noHHO}}} \cdot 100\ \% \right| \quad (13)$$

where $\text{Improve}_{\text{Performance}}$ = Improvement of engine performance (%), such as engine thermal efficiency and AFR error against the commanded AFR.
$\text{Performance}_{\text{HHO}}$ = Performaance of gasoline engine using HHO (%).
$\text{Performance}_{\text{noHHO}}$ = Performnce of gasoline engine without HHO (%).

Meanwhile, improvement of engine torque due to HHO appears on the increment of peak engine torque relative to the applied load on the engine, as shown in Equation (14):

$$\text{Improve}_{\text{torque}} = \left| \frac{(\text{Peak Torque}_{\text{HHO}}\text{-Load}) - (\text{Peak Torque}_{\text{noHHO}}\text{-Load})}{(\text{Peak Torque}_{\text{noHHO}}\text{-Load})} \cdot 100\% \right| \quad (14)$$

where $\text{Improve}_{\text{torque}}$ = Improvement of engine torque (%);
Load = Load applied to the engine (N·m);
$\text{Peak Torque}_{\text{HHO}}$ = Peak torque of gasoline engine using HHO usage (N·m);
$\text{Peak Torque}_{\text{noHHO}}$ = Peak torque of gasoline engine without HHO usage (N·m);

Figures 11 shows the engine torque due to the adaptive HHO flow rate when the engine speed changed from idle speed to 3000 rpm at the 8th second, and a medium load (27.5 N·m) was applied to the engine at the 13th second. The engine torque of a gasoline engine, whether using the fixed HHO flow rate or without HHO, were the same as in Figures 11, except for the peak and steady values.

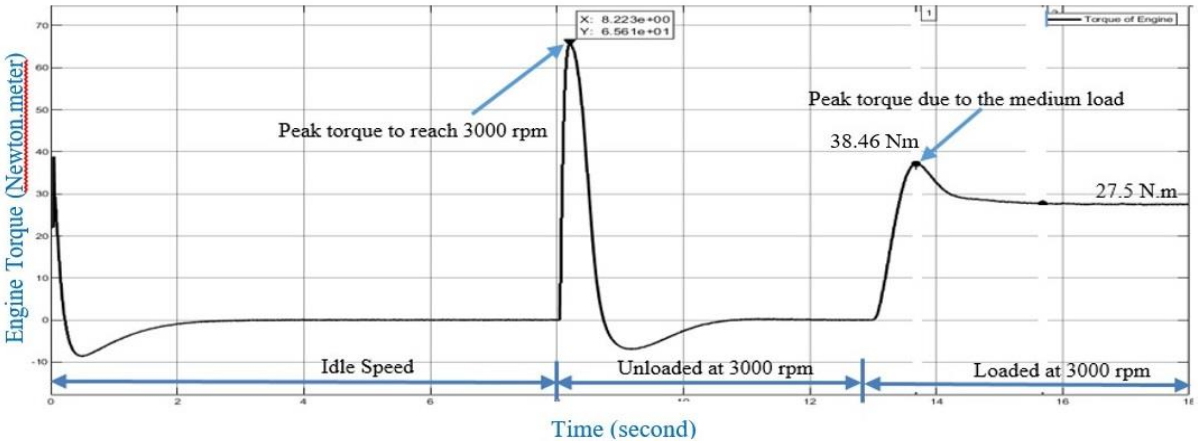

Figure 11 Engine torque of gasoline engine using the adaptive HHO flow rate at 3000 rpm with medium load

Figure 12 Improvement comparison of gasoline engine performance using the fixed and adaptive HHO flow rates at 2500 rpm, various loads and commanded AFRs

Figure 13 Improvement comparison of gasoline engine performance using the fixed and adaptive HHO flow rates at 3000 rpm, various loads and commanded AFRs

Figure 14 Improvement comparison of gasoline engine performance using the fixed and adaptive HHO flow rates at 4000 rpm, various loads and commanded AFRs

4.2.1 Improvement of AFR error against the commanded AFR

Initially, the engine starts with an AFR error of 0.1% against the commanded AFR. Figures 12 - 14 show that only the gasoline engine using the adaptive HHO flow rate improves the steady AFR error against the commanded AFR by 100% during idle speed, unloaded, and loaded engine operation at 2500 rpm, 3000 rpm, and 4000 rpm with the commanded AFR= 12.6, 14.7, and 15.4.

The 100% improvement in steady AFR error, as shown in Figures 12 - 14, occurs because the adaptive HHO controller reduces the AFR error to zero against the commanded AFR by managing the HHO generator's current, so the HHO generator produces a proper HHO flow rate for various engine operations. The adaptive HHO controller works by combining fuzzy logic and polynomial function controls, which involve the engine parameters, such as MAF, AFR*, and the commanded AFR issued by ECU, as described in section 3.4. Moreover, providing the correct amount of hydrogen and oxygen, which compose HHO gas, ensures that the actual AFR* of the engine matches the commanded AFR (target AFR) issued by the ECU, as stated in Equation (7). As a result, the adaptive HHO usage makes the AFR* of the engine achieve the commanded AFR, so the engine torque increases and meets precisely with the required torque to handle any load. Improvement of AFR* also improves engine thermal efficiency, as stated by Equation (9).

In contrast, with the same initial AFR error of 0.1% against the commanded AFR, Figures 12-14 also show that the fixed HHO flow rate method, using 10.07 amperes of the HHO generator's current, improves the AFR error during idle speed, unloaded operation, and small, medium, and big-loaded engine operations by 0%, 0% to 100%, 0% to 100%, 50% to 100%, and 50% to 100%, depending on engine speed and the commanded AFR. Significant improvement in the AFR error occurs at 3000 rpm with a big load operation and at 4000 rpm with a small load operation.

Referring to Equation (13), the small AFR error improvement occurs because the AFR error against the commanded AFR is significant, so the engine cannot reach the commanded AFR. Meanwhile, the significant AFR error occurs because the HHO flow rate is improper (too much) and does not adapt to load and engine speed variations. As stated in Equation (7), the more the HHO gas consisting of hydrogen and oxygen with a 1:8 mass ratio, the greater the AFR* decreases. Conversely, the lesser the HHO gas, the greater the AFR increases. As a result, the actual AFR* cannot achieve the commanded AFR if the HHO flow rate is improper.

Comparing the AFR error improvement due to the fixed and the adaptive HHO flow rates usage on a gasoline engine, it is concluded that the adaptive HHO flow rate due to the proposed controller makes better improvement of the AFR error than that resulted by the fixed HHO flow rate method.

4.2.2 Improvement of Engine Torque

The improvement in engine torque due to HHO is evident in the increase of peak engine torque relative to the applied load on the engine. Figures 12 - 14 show the engine torque improvement referring to Equation (14), which calculates the torque increment against the torque of engine without HHO. Figures 12 -14 show that the improvement of the engine torque due to the adaptive HHO flow rate during small, medium, and big-loaded engine operations, respectively, is 1.5 % - 4.7 %, 6.8 % - 26.8 %, and 21.1 % - 72.8 % depending on engine speed and the commanded AFR. Engine torque improvement due to the adaptive HHO flow rate is always better than the fixed HHO flow rate during the same engine operations because the adaptive HHO controller provide a proper amount of HHO than the fixed HHO flow rate method during engine operations.

Moreover, the adaptive HHO flow rate supplementation results in significant engine torque improvement during big-loaded engine operations. Conversely, only a small engine torque improvement occurs during small-loaded engine operations.

Those phenomena occur because the more the load, the greater the mass airflow (MAF) increases. As a result, the HHO flow rate increases due to the increasing MAF, as described in section 3.4. Then, increasing HHO flow rate increases the engine torque because more hydrogen energy in HHO gas enters the engine, as stated in Equation (6).

In contrast, Figures 12 - 14 also show that the fixed HHO flow rate supplementation in a gasoline engine improves engine torque during small, medium, and big-loaded engine operations by 0% to 0.6%, 0.3% to 14.2%, and 9.3% to 50.1%, respectively, depending on engine speed and the commanded AFR. However, the engine torque improvement due to the fixed HHO flow rate is always less than the adaptive HHO flow rate because the amount of HHO flow rate is improper and does not adapt to engine speed and load variations. Even during small-loaded engine

operations at 2500 rpm and 3000 rpm, the fixed HHO flow rate usage does not improve the engine torque.

The phenomena of an engine using the fixed HHO flow rate above occur because the more the load, the greater the mass airflow (MAF) increases. Meanwhile, combination of the increased MAF, fuel, and the fixed amount of HHO flow rate due to 10.07 Ampere of HHO generator's current makes the AFR of engine achieve the commanded AFR, as Equation (7) stated. As a result, the engine torque optimally increases, so the engine torque improvement is big during big-loaded engine operation.

Conversely, the lesser the load, the greater MAF decreases. Meanwhile, combination of the decreased MAF, fuel, and the fixed amount of HHO flow rate due to 10.07 Ampere of HHO generator's current makes the AFR of engine not achieve the commanded AFR, as stated in Equation (7). As a result, the engine torque does not optimally increase, so the engine torque improvement is small during small-loaded engine operation.

4.2.3 Improvement of Engine Thermal Efficiency

Figures 12 - 14 show that the improvement of engine thermal efficiency due to the adaptive HHO flow rate during small, medium, and big-loaded engine operations, respectively, is 11.5 % - 19.8 %, 11.7 % - 19.8 %, and 11.8 % - 19.9 % depending on engine speed and the commanded AFR. The improvement is calculated based on Equation (13). Significant improvement in engine thermal efficiency occurs at the commanded AFR = 12.6. Increasing the commanded AFR decreases the improvement of engine thermal efficiency. Moreover, Figures 12 - 14 also show that the higher engine speed and bigger loads slightly affect the improvement of engine thermal efficiency. Hence, the improvement of engine thermal efficiency is relatively stable. These phenomena are verified in the following paragraph.

Referring to the definition of engine thermal efficiency and Equation (9), it is clear that engine thermal efficiency depends on engine torque, engine speed, load, amount of HHO gas, new air-fuel ratio (AFR*) due to HHO, and mass airflow (MAF) entering the engine.

When the engine operates at the commanded AFR= 12.6, the value of MAF input is amplified by a big MAF gain factor, which Equation (10) states that the smaller the commanded AFR, the greater the MAF gain increases. As a result, more HHO is generated due to a big MAF value, as described in subsection 3.4.1. The big amount of HHO adds engine torque more due to hydrogen energy composing HHO gas, as stated in Equation (6). Meanwhile, engine torque affects the engine thermal efficiency, as Equation (9) states. That is why the improvement of engine thermal efficiency is big during the commanded AFR = 12.6. Conversely, the bigger the commanded AFR, the greater the MAF gain decreases. As a result, a smaller amount of HHO results, so additional engine torque decreases, which decreases the engine thermal efficiency. That is why the improvement of engine thermal efficiency is smaller during operation with the commanded AFR = 15.4.

Moreover, Figures 12 - 14 also show that the adaptive HHO flow rate usage makes the improvement of engine thermal efficiency slightly change at any change of engine speed and load. This phenomenon occurs because the adaptive HHO controller makes the proper amount of HHO for any engine speed and load variation, so the engine torque is optimal. As a result, the improvement of engine thermal efficiency is relatively stable, although engine speed and load change.

Figures 12 - 14 show that the improvement of engine thermal efficiency due to the fixed HHO flow rate during small, medium, and big-loaded engine operations, respectively, is 11.6 % - 28.9 %, 9.1 % - 20.9 %, and 7.5 % - 16.8 % depending on engine speed and the commanded AFR. Significant improvement in engine thermal efficiency occurs at the commanded AFR = 12.6. Increasing the commanded AFR makes the improvement of engine thermal efficiency slightly decrease. However, Figures 12 - 14 also show that the higher engine speed and the bigger load on engine using the fixed HHO flow rate, make the engine thermal efficiency significantly decrease. These phenomena are verified in the following paragraph.

A gasoline engine has the biggest torque when operating at the commanded AFR = 12.6. Then, the engine torque increases when the fixed HHO flow rate supplementation provides the additional torque due to hydrogen energy contained by HHO gas, as stated in Equation (6). Increasing the commanded AFR decreases the gasoline engine torque but does not change the additional torque from the HHO gas because the amount of HHO gas is fixed. As a result, the total engine torque slightly decreases. Meanwhile, Equation (9) states that engine torque affects the engine thermal efficiency. This is why the improvement of engine thermal efficiency of the engine using the fixed HHO flow rate slightly decreases as the commanded AFR increases.

Moreover, the improvement of engine thermal efficiency also decreases when the load increases. Equation (9) states that a bigger load decreases engine thermal efficiency if the engine torque does not increase. Meanwhile, the additional torque due to the hydrogen energy of HHO is fixed. As a result, total engine torque does not increase, so improvement of engine thermal efficiency decreases.

Besides, the improvement of engine thermal efficiency using the fixed HHO flow rate also decreases when the engine operates at a higher engine speed. A higher engine speed causes smaller duration of intake cycle of the engine to collect air, fuel, and HHO gas. As a result, the engine torque decreases, as stated in Equation (6), so the improvement of engine thermal efficiency decreases.

4.3 Comparison of engine performance improvement due to HHO supplementation

Table 2 summarizes the gasoline engine performance improvements due to HHO usage. The engine performance improvements include AFR error against the commanded AFR, engine torque, and engine thermal efficiency.

Table 2 Comparison of engine performance improvement due to HHO supplementation

Improvement Parameter	Gasoline Engine Performance Using the Adaptive HHO Flow Rate	Gasoline Engine Performance Using the Fixed HHO Flow Rate
AFR error against the commanded AFR	Improves AFR error by 100% for all engine speeds, loads, and the commanded AFRs.	• Improves AFR error by 0% to 100% (uneven) depending on engine speed, load, and the commanded AFR. • Significant AFR error improvement of the AFR error occurs at 3000 rpm with big-loaded operation and at 4000 rpm with small-loaded operation.
Engine torque	• Improves engine torque during small, medium, and big-loaded operations, by 1.5 % to 4.7 %, 6.8 % to 26.8 %, and 21.1 % to 72.8 %, respectively, depending on engine speed and the commanded AFR. • Improves engine torque better than the fixed HHO flow rate usage.	Improves engine torque during small, medium, and big-loaded operations, by 0 % to 0.6 %, 0.3 % to 14.2%, and 9.3 % to 50.1 %, respectively, depending on engine speed and the commanded AFR.
Engine thermal efficiency	• Improves engine thermal efficiency during small, medium, and big-loaded engine operations, by 11.5 % to 19.8 %, 11.7 % to 19.8 %, and 11.8 % to 19.9 %, respectively, depending on engine speed and the commanded AFR. • Improves engine thermal efficiency less than the fixed HHO flow rate usage, but the improvement is relatively stable against changes in engine speed and load. • Significant improvement in engine thermal efficiency occurs at the commanded AFR of 12.6. The improvement significantly changes with changes in the commanded AFR issued by ECU.	• Improves engine thermal efficiency during small, medium, and big-loaded engine operations, by 11.6 % to 28.9 %, 9.1 % to 20.9 %, and 7.5 % to 16.8 % depending on engine speed and the commanded AFR. • Improves engine thermal efficiency more than the adaptive HHO flow rate, but the improvement significantly changes due to changes of engine speed and load. • Significant improvement in engine thermal efficiency occurs at the commanded AFR of 12.6. The improvement is relatively stable with changes in the commanded AFR issued by ECU.

5. Conclusion

The proposed adaptive HHO controller, which works based on the combination of fuzzy logic and polynomial function controls, makes the HHO generator produce the proper amount of HHO gas for any gasoline engine operations by adapting to the actual air-fuel ratio (AFR*) of the engine, mass airflow (MAF) entering the engine, and the commanded AFR issued by ECU. As a result, the proposed adaptive HHO controller improves AFR error against the commanded AFR by 100% for all engine speeds, loads, and the commanded AFRs. In contrast, the fixed HHO flow rate supplementation improves AFR error by 0% to 100% (uneven) depending on engine speed, load, and the commanded AFR. Significant improvement in the AFR error

occurs at 3000 rpm during big-loaded operation and 4000 rpm with a small-loaded operation.

Additionally, the adaptive HHO flow rate supplementation improves engine torque during small, medium, and big-loaded operations, by 1.5 % to 4.7 %, 6.8 % to 26.8 %, and 21.1 % to 72.8 %, respectively, depending on engine speed and the commanded AFR. This improvement of engine torque is better than that achieved with the fixed HHO flow rate usage. On the contrary, the fixed HHO flow rate supplementation improves engine torque during small, medium, and big-loaded operations, by 0 % to 0.6 %, 0.3 % to 14.2 %, and 9.3 % to 50.1 %, respectively, depending on engine speed and the commanded AFR.

The adaptive HHO flow rate supplementation improves engine thermal efficiency during small, medium, and big-loaded engine operations, respectively, by 11.5 % - 19.8 %, 11.7 % - 19.8 %, and 11.8 % - 19.9 %, depending on engine speed and the commanded AFR. The improvement in engine thermal efficiency is lower than with the fixed HHO flow rate, but it remains relatively stable across changes in engine speed and load. Moreover, a significant improvement in engine thermal efficiency occurs at a commanded AFR of 12.6. The improvement varies significantly with changes in the commanded AFR issued by the ECU. On the contrary, the fixed HHO flow rate supplementation improves engine thermal efficiency during small, medium, and big-loaded engine operations, by 11.6 % to 28.9 %, 9.1 % to 20.9 %, and 7.5 % to 16.8 %, respectively, depending on engine speed and the commanded AFR. The improvement in engine thermal efficiency is greater than the adaptive HHO flow rate, but the improvement significantly changes due to changes in engine speed and load. Moreover, significant improvement in engine thermal efficiency occurs at the commanded AFR of 12.6. The improvement is relatively stable against the change of the commanded AFR issued by ECU.

The success in optimally improving the air-fuel ratio, engine torque, and engine thermal efficiency occurs because the proposed adaptive HHO gas controller, which combines fuzzy logic and polynomial function controls to accurately manage the HHO flow rate for a gasoline engine by considering the engine parameters. The novelty of the proposed HHO controller lies in its ability to adapt the HHO flow rate to variations in load and engine speed. Besides, the proposed adaptive controller improves flaws of the previous fixed HHO flow rate method, which causes non-optimal improvement of AFR error, engine torque, and engine thermal efficiency.

For future work, the research needs to explore the electronics-embedded system design and implementation of the adaptive HHO controller by referring to the proposed model. The adaptive HHO controller has the OBD-II interface to obtain real-time data of MAF, actual AFR, and the commanded AFR from ECU.

7. Acknowledgements

The authors thank the Faculty of Electrical Technology and Engineering of Universiti Teknikal Malaysia Melaka in Melaka, Malaysia, and the Department of Electrical Engineering of Universitas Nasional in Jakarta, Indonesia, for the research facilities.

8. References

Abdullah, M. Y. (2015). *Analysis the Using of HHO Related with Fuel Motor Performance* [Master thesis]. Institut Teknologi Sepuluh Nopember, Surabaya, Indonesia.

Aghahasani, M., Gharehghani, A., Mahmoudzadeh Andwari, A., Mikulski, M., Pesyridis, A., Megaritis, T., & Könnö, J. (2022). Numerical Study on Hydrogen-Gasoline Dual-Fuel Spark Ignition Engine. *Processes*, *10*(11), 1-15. https://doi.org/10.3390/pr10112249

Baltacıoğlu, M. K. (2019). A Novel Application of Pulse Width Modulation Technique on Hydroxy Gas Production. *International Journal of Hydrogen Energy*, *44*(20), 9726–9734. https://doi.org/10.1016/j.ijhydene.2018.10.228

Bai, Y. (2013). *Studies on SI engine simulation and air/fuel ratio control systems design* [Doctoral dissertation]. Brunel University School of Engineering and Design, London.

Bogdan, D., Marek, W., Jozinkiewicz, D., Zakrzewski, S., Kaczmarek, M., Binkowski, D., ... & Krzysztof, S. (2023). Research of Dynamic Phenomena in a Model Engine Stand. *Open Engineering*, *13*(1), Article 20220436. https://doi.org/10.1515/eng-2022-0436

Conker, C. (2019). A novel fuzzy logic based safe operation oriented control technique for driving HHO dry cell systems based on PWM duty cycle. *International Journal of Hydrogen Energy*, *44*(20), 9718–9725. https://doi.org/10.1016/j.ijhydene.2018.10.243

Conker, C., & Baltacioglu, M. K. (2020). Fuzzy Self-Adaptive PID Control Technique for Driving HHO Dry Cell Systems. *International Journal of Hydrogen Energy*, *45*(49), 26059–26069. https://doi.org/10.1016/j.ijhydene.2020.01.136

El Soly, A. K., Gad, M. S., & El Kady, M. A. (2023). Experimental Comparison of Oxyhydrogen Production Rate Using Different Designs of Electrolyzers. *International Journal of Hydrogen Energy*, *48*(93), 36254–36270. https://doi.org/10.1016/j.ijhydene.2023.06.022

Elsemary, I. M. M., Attia, A. A. A., Elnagar, K. H., & Elsaleh, M. S. (2017). Spark timing effect on performance of gasoline engine fueled with mixture of hydrogen–gasoline. *International Journal of Hydrogen Energy*, *42*(52), 30813–30820. https://doi.org/10.1016/j.ijhydene.2017.10.125

Gad, M. S., El-Shafay, A. S., Ağbulut, Ü., & Panchal, H. (2024). Impact of produced oxyhydrogen gas (HHO) from dry cell electrolyzer on spark ignition engine characteristics. *International Journal of Hydrogen Energy*, *49*, 553–563. https://doi.org/10.1016/j.ijhydene.2023.08.210

Gambou, F., Guilbert, D., Zasadzinski, M., & Rafaralahy, H. (2022). A Comprehensive Survey of Alkaline Electrolyzer Modeling: Electrical Domain and Specific Electrolyte Conductivity. *Energies*, *15*(9), 1–20. https://doi.org/10.3390/en15093452

Huang, H. (2023). PI Control Technology Principal Analysis and Simulation. *Highlights in Science, Engineering and Technology*, *71*, 104–111. https://doi.org/10.54097/hset.v71i.12676

Karn, S. K., & Demiroglu, N. (2023). A Theoretical Study on Energy of a Gaseous System Vis-a-Vis Mass and Temperature. *Journal of Electronics Cooling and Thermal Control*, *12*(01), 1–8. https://doi.org/10.4236/jectc.2023.121001

Khajepour, A., Fallah, S., & Goodarzi, A. (2014). Electric and Hybrid Vehicles - Technologies, Modeling and Control: A Mechatronic Approach. In *John Wiley & Sons, Ltd: Vol. Chapter 1* (First Edit). John Wiley & Sons, Ltd. https://doi.org/10.1007/978-3-7091-2926-5_1

Kultsum, U., Soumi, A. I., Baharudin, A., & Manunggal, P. D. (2024). Performance Assessment of Spark-Ignition Engine Combined with an HHO Generator. *Engineering Proceedings*, *63*(3), 1-9. https://doi.org/10.3390/engproc2024063003

Lim, J. H., Hou, J., Chun, J., Lee, R. D., Yun, J., Jung, J., & Lee, C. H. (2022). Importance of Hydroxide Ion Conductivity Measurement for Alkaline Water Electrolysis Membranes. *Membranes*, *12*(6), 1-12. https://doi.org/10.3390/membranes12060556

Madyira, D. M., & Harding, W. G. (2014, January 14-16). Effect of HHO on four stroke petrol engine performance [Conference presentation]. *9th South African Conference on Computational and Applied Mechanics, South Africa*. https://core.ac.uk/download/pdf/54204275.pdf

Marefatjouikilevaee, H., Auger, F., & Olivier, J. C. (2023). Static and Dynamic Electrical Models of Proton Exchange Membrane Electrolysers: A Comprehensive Review. *Energies*, *16*(18), 1–36. https://doi.org/10.3390/en16186503

Musmar, S. A., & Al-Rousan, A. A. (2011). Effect of HHO gas on combustion emissions in gasoline engines. *Fuel*, *90*(10), 3066-3070. https://doi.org/10.1016/j.fuel.2011.05.013

Muthu, V. S. S., Osman, S. A., & Osman, S. A. (2022). A Review of the Effects of Plate Configurations and Electrolyte Strength on Production of Brown Gas Using Dry Cell Oxyhydrogen Generator. *Journal of Advanced Research in Fluid Mechanics and Thermal Sciences*, *99*(1), 1-8. https://doi.org/10.37934/arfmts.99.1.18

Na, J., Chen, A. S., Huang, Y., Agarwal, A., Lewis, A., Herrmann, G., Burke, R., & Brace, C. (2021). Air-Fuel Ratio Control of Spark Ignition Engines with Unknown System Dynamics Estimator: Theory and Experiments. *IEEE Transactions on Control Systems Technology*, *29*(2), 786–793. https://doi.org/10.1109/TCST.2019.2951125

Nabil, T. (2019). Efficient Use of Oxy-hydrogen Gas (HHO) in Vehicle Engines. *Journal Europeen Des Systemes Automatises*, *52*(1), 87–96. https://doi.org/10.18280/jesa.520112

Namitha, S., & Shantharama, R. (2013). Fuzzy Logic Controller for the Speed Control of an IC Engine using Matlab \ Simulink. *International Journal of Recent Technology and Engineering (IJRTE)*, *2*(2), 124–127.

Newborough, M., & Cooley, G. (2021). Green Hydrogen: The Only Oxygen and Water Balanced Fuel. *Fuel Cells Bulletin*, *2021*(3), 16–19. https://doi.org/10.1016/S1464-

2859(21)00169-3

Niroula, S., Chaudhary, C., Subedi, A., & Thapa, B. S. (2023). Parametric Modelling and Optimization of Alkaline Electrolyzer for the Production of Green Hydrogen. *IOP Conference Series: Materials Science and Engineering*, *1279*(1), 012005. https://doi.org/10.1088/1757-899x/1279/1/012005

Ridhuan, A., Osman, S. A., Fawzi, M., Alimin, A. J., & Osman, S. A. (2021). A Review of Comparative Study on The Effect of Hydroxyl Gas in Internal Combustion Engine (ICE) On Engine Performance and Exhaust Emission. *Journal of Advanced Research in Fluid Mechanics and Thermal Sciences*, *87*(2), 1-16. https://doi.org/10.37934/arfmts.87.2.116

Ridhwan, A. M., Mansor, M. R., Tamaldin, N., Latief, F. H., & Repi, V. V. R. (2023). Effect of KOH Concentration on the Performance of HHO Generator at Varying Plate Surface Textures. *Journal of Advanced Research in Fluid Mechanics and Thermal Sciences*, *106*(2), 116–128. https://doi.org/10.37934/arfmts.106.2.116128

Setiadi, H., Jones, K. O., Nugroho, T. A., Abdillah, M., Trilaksana, H., & Amrillah, T. (2021). Design of Spark Ignition Engine Speed Control Using Bat Algorithm. *International Journal of Electrical and Computer Engineering*, *11*(1), 794–801. https://doi.org/10.11591/ijece.v11i1.pp794-801

Sudarmanta, B., Darsopuspito, S., & Sungkono, D. (2016). Application of Dry Cell HHO Gas Generator with Pulse Width Modulation on Sinjai Spark Ignition Engine Performance. *International Journal of Research in Engineering and Technology*, *5*(2), 105-112. https://doi.org/10.15623/ijret.2016.0502019

The MathWorks Inc. (2024). *Engine Timing Model with Closed Loop Control*. Retrived Febuary 2, 2024 from https://www.mathworks.com/help/simulink/slref/engine-timing-model-with-closed-loop-control.html

Yilmas, A. C. (2010). *Design and Applications of Hydroxy (HHO) System* [Master thesis]. Cukurova University - Institute of Natural and Applied Sciences, Adana, Turkeye. http://libratez.cu.edu.tr/tezler/7998.pdf